RESEARCH ARTICLE

Removal of Cr (III) by using Chitosan-Grafting-Poly(Acryl Acid-Crotonic Acid) Characterization and Kinetic Study

Rasha A. Mohammed[1*], Hazim A. Walli[2]

[1]*Department of Chemistry, College of Education, University of Al-Qadisiyah, Iraq.*
[2]*Department of Ecology, College of Science, University of Al-Qadisiyah, Iraq.*

Received: 01st April, 2023; Revised: 22th July, 2023; Accepted: 17th August, 2023; Available Online: 25th September, 2023

ABSTRACT

Hydrogel nanocomposites were prepared using free radical polymerization chitosan and acrylic acid (AA) in combination with crotonic acid. KPS was employed as the initiating agent, while MBA functioned as the cross-linking agent. The nanocomposite of Ch-g-P(AA-co-CA) is a powerful pollutant absorber. Cr (III) was removed from the water using the combination. Field emission scanning electron microscopy (FESEM) and infrared spectroscopy (FTIR) were used to examine the nanocomposites' structure and morphology. The kinetics of Cr (III) adsorption was studied using these rates. Pseudo-second order kinetics characterize the adsorption process. Hydrogel nanocomposite efficiently removes Cr by adsorption (III).

Keywords: Chitosan, Adsorption, Acrylic acid, Cr (III), Crotonic acid.

International Journal of Pharmaceutical Quality Assurance (2023); DOI: 10.25258/ijpqa.14.3.35

How to cite this article: Mohammed RA, Walli HA. Removal of Cr (III) by using Chitosan-Grafting-Poly(Acryl Acid-Crotonic Acid) Characterization and Kinetic Study. International Journal of Pharmaceutical Quality Assurance. 2023;14(3):671-674.

Source of support: Nil.

Conflict of interest: None

INTRODUCTION

Water's critical role in sustaining life has been universally recognized.[1] With the surge in industrial activities, amplified human exploitation of natural resources, and escalated mining operations, contaminants have been ingested into water sources, leading to pronounced water pollution.[2-4] Heavy metals in wastewater, including elements like Cr, Cd, Ni, and Pb, have garnered attention due to their heightened toxicity levels.[5] For instance, lead's interference with cellular components can disrupt their functioning,[6] manifesting symptoms such as dizziness, pronounced fatigue, and depression. The imperative to purge these contaminants has posed considerable challenges.[7] Various strategies like ion exchange, electrodeposition, and membrane filtration have been deployed for heavy metal extraction from polluted waters, yet these methods are not without shortcomings.[8-11] The adsorption technique stands out for its quick action and selectivity in removing metal ions from contaminated water sources.[12-14]

MATERIALS AND METHODS

Chemicals and Materials

Crotonic acid (CA), chitosan (Ch), acrylic acid (AA), N,N'-Methylene-bis-acrylamide (MBA), and potassium persulfate were among the compounds utilized, all of which were of the highest analytical grade. Additionally, a solution of Cr (III) was prepared. For the preparation of all solutions, deionized water was employed.

Synthesis of Ch-g-P(AA-co-CA) Hydrogel Nano composite

The synthesis of Ch-g P(AA-CA) involved a specific procedure using Ch, AA, and CA. Initially, 1.0 g of Ch was dissolved in 40 mL of a 2% of CH_3COOH solution and stirred mechanically for 30 minutes. Following a 30-minute nitrogen purge to eliminate dissolved oxygen, 10 mL of AA and 1.0 g of CA dissolved in 10 mL were introduced into the mixture. Subsequently, the solution's temperature was elevated to 60°C. Recently prepared solutions of (0.1 g in 4 mL) MBA and (0.1 g in 4 mL) KPS were added. The mixture was maintained at 60°C using a three-hour water bath. Post this duration, the samples were subjected to baking at 60°C until a consistent weight was achieved. The resulting test samples were ground to achieve a particle size finer than 75 µm. The same method was used to produce Ch-g-P(AA-co-CA) (Figure 1).

Characterization of Ch-g-P(AA-co-CA) Hydrogel

FTIR spectroscopy

Hydrogels were analyzed using infrared spectroscopy (FTIR Shimadzu8400S, Japan) to classify the functional groups of Ch-g-P(AA-co-CA) hydrogels. Data for the generated surface were obtained via Fourier transform infrared spectroscopy (FTIR) using potassium bromide (KBr) in the wavelength range (4000–400 cm^{-1}).

**Author for Correspondence: nadhir.dhaman@qu.edu.iq*

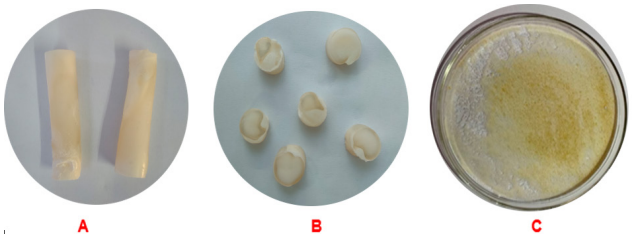

Figure 1: Photograph of: (A) preparing and cutting (B) washing (C) drying and grinding of hydrogel

Field emission scanning electron microscopy

FESEM was used to compare the nano-hydrogel composite's morphology before and after loading with titanium dioxide at various magnification levels.

Calibration curves of Cr (III) ions

The Cr (III) calibration curve was established using atomic absorption spectrometry. Standard solutions of lead ion, with concentrations spanning from 1 to 100 mg/L, were utilized for this determination. The outcomes indicated that the ion adhered to the Beer-Lambert law (Figure 2).[15]

Kinetic studies

This study determined the equilibrium time by dissolving 0.1 g of adsorbent in 20 mL of a standard lead ion solution at 25°C using a thermostatic shaker. Fluids were separated using a centrifuge, and equilibrium time was determined by measuring absorbance with an atomic absorption device.

RESULTS AND DISCUSSION

FTIR Analysis

As FTIR spectrum shows in Figure 3, the permeability decreases at the adsorption peaks after Cr(III) adsorption on the surface, suggesting that Cr(III) ions have bonded with amino groups and altered their vibration. Additionally, hydroxyl, amine, and carbonyl groups shift positions as a result of Pb ion adsorption, as evidenced by an increase in OH group size and a decrease in C-H group bending. The FTIR bands at 1493 cm^{-1} are assigned to the C=O, amide group, 2800 cm^{-1} to the CH_3 stretching group, 1735 cm^{-1} to the -C=O of COOH, and 1396 cm^{-1} to the -C=C group.[16-19]

FESEM

Through the utilization of the FESEM technique, in-depth insights into the surface characteristics, including particle form, dimensions, consistency among compound elements, surface dispersion, polymer chain linkages, and the inherent surface nature (porous vs. smooth) were obtained. The hydrogel[20] was identified as a nanocomposite characterized by its spongy-like, porous, and rough stratified texture. Figure 4 offers visual evidence of the hydrogel's surface, marked by arbitrary wrinkle formations. Yet, a noteworthy transformation was discerned following the adsorption of Pb ions; the FESEM images portrayed a shift to a more unified and refined surface. This suggests the infiltration of Pb ions into the surface voids.[21,22] Such findings, clearly demonstrated in Figure 4,

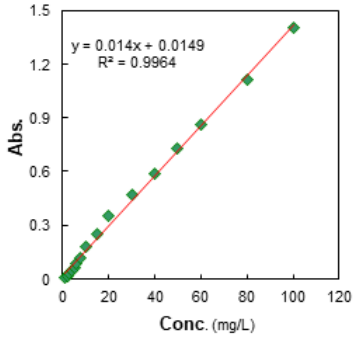

Figure 2: Calibration Curves of Cr (III) Ions

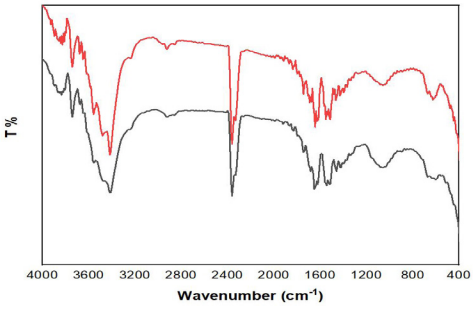

Figure 3: The FTIR spectrum after cr (iii) adsorption process

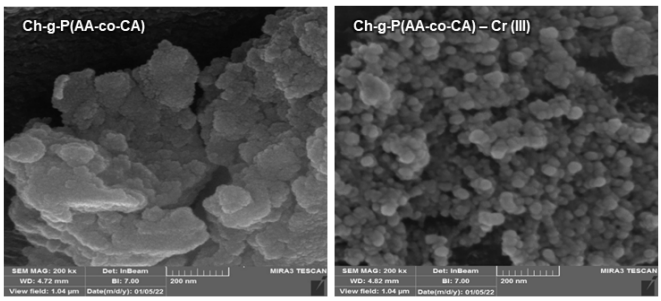

Figure 4: FESEM Images of the overlapping surface of Ch-g-P(AA-co-CA) before and after adsorption Cr (III)

validate the adsorption phenomenon.[5] An auxiliary proof of the adsorption process's efficiency is encapsulated in Figure 4, which juxtaposes the oxygen and carbon ratio dynamics of the hydrogel assembly before and after the adsorption phase.[6]

Adsorption Kinetics

The Ch-g-P(AA-co-CA) nanocomposite hydrogel demonstrates adsorptive capabilities towards Cr (III). As illustrated in Figure 5, the relationship with contact duration is evident. The initial stages display an accelerated rate of ion adsorption onto the Ch-g-P(AA-co-CA) nanocomposite, which subsequently diminishes, stabilizing nearly constant post the 120-minute mark. This behavior suggests an abundance of available adsorption sites during the early phases, which might reach saturation as the process unfolds.[23]

Adsorption kinetic studies for Cr(III) ions onto Ch-g-P(AA-co-CA) were conducted by contrasting the pseudo-first-order and pseudo-second-order models. As illustrated in Figure 6 and elaborated upon in Table 1, it was observed that

Table 1: Kinetic Adsorption Coefficients of Pb on Ch-g-P(AA-co-CA) at 25°C

Pseudo- first order Cr (III) on Ch-g-P(AA-co-CA)					
Slope	*intercept*	*k1*	*qe*	*R^2*	
-0.0368	3.2773	0.0368	26.50411	0.9152	
Pseudo - second order Cr (III) on Ch-g-P(AA-co-CA)					
Slope	intercept	qe	k2	h	R^2
0.0286	0.3312	34.96503	0.00247	3.019324	0.9965

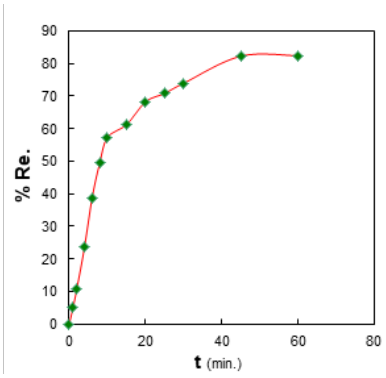

Figure 5: Effect of contact time of removal Cr (III) at 25ºC

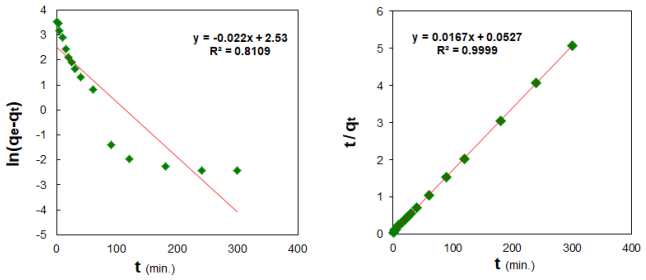

Figure 6: (a) Pseudo-First-order model desorption Cr (III) on Ch-g-P(AA-co-CA) and (b) Pseudo-second-order model adsorption Cr (III) on Ch-g-P(AA-co-CA) at 25°C

the pseudo-second-order model manifested a notably elevated correlation coefficient (R^2=0.9965) when juxtaposed with the pseudo-first-order model. Such findings indicate that the pseudo-second-order model more precisely delineates the underlying adsorption process.

CONCLUSION

The results of the study showed first, the adsorbent compound (Ch-g-P(AA-co-CA)) efficiently removes Cr (III) ions from water. The equilibrium time for chromium (III) ion adsorption is 120 minutes. Adsorbent composite Ch-g-P(AA-co-CA) should be 0.05 g in the Cr (III) adsorption process, step 3. In order to explain the adsorption of Cr (III) on the surface of the Ch-g-P(AA-co-CA) composite, the pseudo-second-rider model is employed.

REFERENCES

1. Zhou Q, Yang N, Li Y, Ren B, Ding X, Bian H, et al. Total concentrations and sources of heavy metal pollution in global river and lake water bodies from 1972 to 2017. Global Ecology and Conservation. 2020;22:e00925.
2. Hong Y-j, Liao W, Yan Z-f, Bai Y-c, Feng C-l, Xu Z-x, et al. Progress in the research of the toxicity effect mechanisms of heavy metals on freshwater organisms and their water quality criteria in China. Journal of chemistry. 2020;2020.
3. Valian M, Salavati-Niasari M, Ganduh SH, Abdulsahib WK, Mahdi MA, Jasim LS. Sol-gel auto-combustion synthesis of a novel chitosan/Ho2Ti2O7 nanocomposite and its characterization for photocatalytic degradation of organic pollutant in wastewater under visible illumination. International Journal of Hydrogen Energy. 2022.
4. Kianipour S, Razavi FS, Hajizadeh-Oghaz M, Abdulsahib WK, Mahdi MA, Jasim LS, et al. The synthesis of the P/N-type NdCoO3/g-C3N4 nano-heterojunction as a high-performance photocatalyst for the enhanced photocatalytic degradation of pollutants under visible-light irradiation. Arabian Journal of Chemistry. 2022;15(6):103840.
5. Mohammadian S, Krok B, Fritzsche A, Bianco C, Tosco T, Cagigal E, et al. Field-scale demonstration of in situ immobilization of heavy metals by injecting iron oxide nanoparticle adsorption barriers in groundwater. Journal of Contaminant Hydrology. 2021;237:103741.
6. Gebretsadik H, Gebrekidan A, Demlie L. Removal of heavy metals from aqueous solutions using Eucalyptus Camaldulensis: An alternate low cost adsorbent. Cogent Chemistry. 2020;6(1):1720892.
7. Rosset M, Sfreddo LW, Perez-Lopez OW, Feris LA. Effect of concentration in the equilibrium and kinetics of adsorption of acetylsalicylic acid on ZnAl layered double hydroxide. Journal of Environmental Chemical Engineering. 2020;8(4):103991.
8. Yang M, Huang Y, Cao H, Lin Y, Cheng X, Wang X. A novel polymeric adsorbent by a self-doped manner: synthesis, characterization, and adsorption performance to phenol from aqueous solution. Polymer Bulletin. 2016;73(8):2321-41.
9. Terzyk AP. Further insights into the role of carbon surface functionalities in the mechanism of phenol adsorption. Journal of colloid and interface science. 2003;268(2):301-29.
10. Ricordel S, Taha S, Cisse I, Dorange G. Heavy metals removal by adsorption onto peanut husks carbon: characterization, kinetic study and modeling. Separation and purification Technology. 2001;24(3):389-401.
11. Khorasanizadeh MH, Hajizadeh-Oghaz M, Khoobi A, Ganduh SH, Mahdi MA, Abdulsahib WK, et al. Synthesis and characterization of HoVO4/CuO nanocomposites for photodegradation of methyl violet. International Journal of Hydrogen Energy. 2022.
12. Wadhawan S, Jain A, Nayyar J, Mehta SK. Role of nanomaterials as adsorbents in heavy metal ion removal from waste water: A review. Journal of Water Process Engineering. 2020;33:101038.
13. Vunain E, Mishra AK, Mamba BB. Dendrimers, mesoporous silicas and chitosan-based nanosorbents for the removal of heavy-metal ions: a review. International journal of biological macromolecules. 2016;86:570-86.
14. Abdulsahib WK, Sahib HH, Mahdi MA, Jasim LS. Adsorption Study of Cephalexin Monohydrate Drug in Solution on Poly (vinyl pyrrolidone-acryl amide) Hydrogel Surface. International Journal of Drug Delivery Technology. 2021;11(4):1169-72.
15. Kolsuz Ozcetin H, Surmelioglu D. Effects of bleaching gel containing TiO2 and chitosan on tooth surface roughness, microhardness and colour. Australian Dental Journal.

2020;65(4):269-77.
16. Wang Y, Zeng L, Ren X, Song H, Wang A. Removal of methyl violet from aqueous solutions using poly (acrylic acid-co-acrylamide)/attapulgite composite. Journal of Environmental Sciences. 2010;22(1):7-14.
17. Farghali AA, Abdel Tawab HA, Abdel Moaty SA, Khaled R. Functionalization of acidified multi-walled carbon nanotubes for removal of heavy metals in aqueous solutions. Journal of Nanostructure in Chemistry. 2017;7(2):101-11.
18. Beauchamp J. Infrared Tables (short summary of common absorption frequencies). 2004.
19. Alpert NL, Keiser WE, Szymanski HA. IR: theory and practice of infrared spectroscopy: Springer Science & Business Media; 2012.
20. Farré M, Barceló D. Introduction to the analysis and risk of nanomaterials in environmental and food samples. Comprehensive analytical chemistry. 59: Elsevier; 2012. p. 1-32.
21. Bloor J, Handy R, Awan S, Jenkins D. Graphene oxide biopolymer aerogels for the removal of lead from drinking water using a novel nano-enhanced ion exchange cascade. Ecotoxicology and Environmental Safety. 2021;208:111422.
22. Thakur S, Verma A, Raizada P, Gunduz O, Janas D, Alsanie WF, et al. Bentonite-based sodium alginate/dextrin cross-linked poly (acrylic acid) hydrogel nanohybrids for facile removal of paraquat herbicide from aqueous solutions. Chemosphere. 2022;291:133002.
23. Aljeboree AM, Mohammed RA, Mahdi MA, Jasim LS, Alkaim AF. Synthesis, Characterization of P(CH/AA-co-AM) and Adsorptive Removal of Cr(III) ions from Aqueous Solution: Thermodynamic Study. NeuroQuantology: An Interdisciplinary Journal of Neuroscience and Quantum Physics. 2021;19:137+.